Energy & Environmental Science

PAPER

View Article Online
View Journal | View Issue

Cite this: *Energy Environ. Sci.*, 2016, 9, 2453

Dye-sensitized solar cells with inkjet-printed dyes†

Syed Ghufran Hashmi,[a] Merve Özkan,[b] Janne Halme,*[a] Shaik Mohammed Zakeeruddin,[c] Jouni Paltakari,[b] Michael Grätzel[c] and Peter D. Lund[a]

Received 18th March 2016,
Accepted 9th June 2016

DOI: 10.1039/c6ee00826g

www.rsc.org/ees

The slow process in which the light absorbing dye molecules are adsorbed from solution on the nanocrystalline TiO_2 photoelectrode film has been a handicap to the fast and cost-effective fabrication of dye-sensitized solar cells (DSSCs) using printing techniques. Here, we report a versatile dye sensitization process, achieved by inkjet printing a concentrated dye solution over the TiO_2 film, which produces solar cells with equal performance and stability as obtained using the popular dye drop casting method. In addition to allowing precise control of dye loading required for dispensing just the right amount of dye to achieve uniform and full coloration of the TiO_2 films without any need for washing off the excess dye, inkjet printing also makes it possible to freely adjust the amount and position of the dye to create DSSCs with tailored transparency, color density gradients, and patterns of one or more dyes on the same electrode. The method was confirmed to be applicable also for non-transparent, high-efficiency DSSC designs that employ a light scattering layer. The inkjet-dyed DSSCs exhibited high stability, retaining almost 100% of their conversion efficiency (η = 6.4 ± 0.2%) and short circuit current density (J_{SC} = 14.2 ± 0.6 mA cm^{-2}) when subjected to a 1000 h accelerated aging test under 1 Sun illumination at 35 °C, followed by additional 1154 hours under 0.5 Sun at 60 °C. These results overcome one of the main hurdles in realizing fully printed DSSCs and open opportunities for entirely new DSSC designs.

Broader context

Dye-sensitized solar cells (DSSCs) can be possibly produced at low cost using high throughput methods such as screen or inkjet printing, but to do so requires re-designing some of their conventional fabrication steps. One of them is the step where the light absorbing dyes are attached to the nanocrystalline TiO_2 photoelectrode. This is normally done on the laboratory scale by slowly soaking the TiO_2 film in a dye solution. Although methods exist to speed up the process from hours to minutes, it could be even quicker and consume less materials, if the dye could be simply printed on the TiO_2 film. We report here for the first time that this can in fact be done using inkjet printing, which at the same time brings about additional benefits. Inkjet dyeing not only simplifies the overall fabrication and consumes less solvents, but also opens new opportunities for creating multi-coloured solar cells with tailored transparency and decorative designs, which can be important attributes for the commercialization of DSSCs.

1. Introduction

Dye sensitized solar cells (DSSCs) have been considered as a promising photovoltaic technology because they can be produced from abundantly available raw materials on various substrates using fast printing processes,[1–3] and have intrinsic features, such as semi-transparency and color,[4,5] as well as good operation at low light intensity,[6] which offer interesting product opportunities for building integrated photovoltaics and energy harvesting for low power wireless electronics.[5,7–9] However, in order to manufacture them at high speed and using the roll-to-roll printing methods, some of their conventional fabrication steps have to be re-designed.[1]

In the conventional fabrication method of dye-sensitized solar cells, a monolayer of dye molecules is attached to the nanocrystalline TiO_2 photoelectrode film by soaking it for 16–24 hours in a dye bath containing the sensitizer molecules, usually the ruthenium complex N719, which is followed by rinsing off the excess dye.[10,11] Although suitable for small-scale experiments, and therefore popular in the research labs, this process is too slow for high through-put manufacturing, which should ideally consist of only fast, additive material printing and deposition steps, each completed in the time frame of seconds to minutes, as already demonstrated for roll-to-roll fabrication of organic solar cells.[12–17]

[a] Department of Applied Physics, Aalto University School of Science, P.O. BOX 15100, FI-00076 Aalto (Espoo), Finland. E-mail: janne.halme@aalto.fi
[b] Department of Forest Products Technology, Aalto University School of Chemical Technology, P.O. BOX 15100, FI-00076 Aalto (Espoo), Finland
[c] Laboratory of Photonics and Interfaces, Ecole Polytechnique Federale de Lausanne (EPFL), CH G1 551, Station 6, CH-1015 Lausanne, Switzerland

† Electronic supplementary information (ESI) available. See DOI: 10.1039/c6ee00826g

Studies show that the time required for saturating the surface of TiO_2 with the N719 dye can be shortened down to three minutes[18] either by using a more concentrated dye solution,[18–20] performing the sensitization at higher temperature,[20,21] or by facilitating the supply of the dye molecules from the solution into the mesoporous film by circulating[20–22] or sonicating[23] the dye solution, by applying an electrical field,[24] or even by mixing the TiO_2 nanoparticles into the concentrated dye solution followed by spraying.[25] The adsorption kinetics depend also on the chemical conditions of the TiO_2 surface, which can be altered to be more favorable for dye adsorption by treating it with acidic solution.[26] For small area DSSCs, the fastest reported uptake of N719 through the soaking process was completed in 5–10 minutes using drop casting and pumping methods, which gave dyed TiO_2 photoelectrodes capable of producing 11–18 mA cm^{-2} short circuit current density under the standard reporting conditions.[18–20]

On the other hand, the sensitization studies of large surface area DSSC modules are few, and among them the popular scheme has been the dye circulation through a pump,[21,22,27] however, the sensitization time through this circulation technique was long (more than two hours). In the case of the new concept of pre-sensitization of TiO_2 nanoparticles in the dye solution followed by spraying, reported recently for large area flexible DSSCs, material consumption may be an issue since a significant fraction of the sprayed material can be wasted over the non-active area, which can increase the overall production cost.[25]

Since most of the active materials of DSSCs can be deposited by printing and coating,[1,28] it would be advantageous from the point-of-view of manufacturing if the dye could also be simply printed on the TiO_2 films. The first steps toward this direction were taken by Nazeeruddin *et al.* who introduced a rapid sensitization technique, in which a known volume of a highly concentrated N719 dye solution is pipetted onto the TiO_2 electrode, or the electrode is immersed in it briefly.[18] This process, which took only three minutes at the shortest,[18] was thereafter followed by others who showed that a similar performance can be achieved with fast sensitization as with the traditional sensitization technique.[19,20,29] Nevertheless, in some of these studies, the excess, non-adsorbed dye was washed away afterwards,[18,29] which suggests that the control of the applied amount of dye was not sufficiently accurate to dispense just enough dye to saturate the film, but not more. Clearly, the rapid sensitization could reach its full potential as a DSSC fabrication process only if it could be performed using a precise, automated and industrially scalable printing technique.

Here, we report a versatile dye sensitization process, achieved through the inkjet printing of concentrated dye solutions over the TiO_2 electrode films (Fig. 1), which allows accurate control of the printed amount of dye, while producing solar cells with equal performance and stability as obtained using the known drop casting process. Based on the piezo-electric 'drop-on-demand' deposition of nominal 10 picoliter sized droplets, inkjet printing not only allows dispensing the right amount of dye needed for uniform and full coloration of the TiO_2 films without the excess dye, but also makes it possible to freely adjust the dye loading to create solar cells with tailored transparency, color density gradients, and arbitrary patterns of one or multiple dyes on the same TiO_2 electrode (Fig. 1).

The dye was printed using an automated inkjet printer (Fuji Film's Dimatix Material Printer, model DMP-2800 Series) by filling the concentrated dye solutions (10–16 mM in DMF or DMSO) into its polymer cartridge after passing them through a 0.2 μm filter (see the Experimental section for further details). In the following, we discuss first the results from semi-transparent DSSCs, obtained by the inkjet printing of a ruthenium sensitizer C101.[32]

2. Results and discussion

The following discussion has been divided into two parts (Sections 2 and 3). In the first part, we demonstrated the

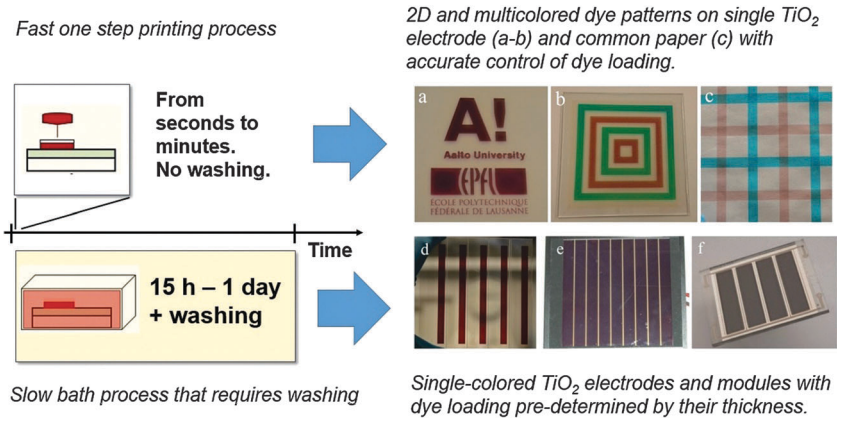

Fig. 1 An Illustration of DSSC fabrication using old and new dye sensitization methods (a) 2D patterning demonstration of Aalto University and EPFL University logos using the inkjet printing technique used in this study from a concentrated dye solution of C101 dye over a nanocrystalline TiO_2 layer (b) colorful patterns (SQ2 dye in green and Z907 dye in red) can be obtained on a single substrate which cannot be realized using the old dye bath technique (c) overlapping prints of SQ2 and Z907 dyes on a regular office paper as a demonstration of co-sensitization and color tuning (d–f) large area sensitized electrodes fabricated using the traditional dye bath methods.[30,31]

potential capabilities of inkjet printing by using the semi-transparent DSSCs produced through efficient control of dye loadings on nanocrystalline mesoporous TiO_2 layers (no scattering layers were employed), whereas in the second part, the stability of printed dye is investigated in the standard DSSCs employing the scattering TiO_2 layers.

2.1. Demonstration of the capabilities of inkjet printing of the dye

2.1.1. Variable transparency, color density gradients and multi-dye patterns in a single DSSC. One of the advantages of inkjet printing is the controlled dispensing of fluid through which the dye loading of the photoelectrode can be accurately controlled. To demonstrate this capability, and to determine the printing parameters that yield full coloration, a 10 mM solution of C101 dye in DMF was inkjet-printed 1–5 times (1.1 μL cm^{-2} per print) over a 7 μm thick TiO_2 electrode (0.4 cm^2, without a scattering layer) using 10 pL drop volume and 30 μm drop spacing, which corresponds to 11.3 nmol cm^{-2} of dispensed dye per print. After a settling period of *ca.* 1 minute, during which the dye attached on the TiO_2 surface from the printed solution, the films were rinsed with DMF ("washed" samples) to remove the possible non-adsorbed dye, or the rinsing step was omitted ("non-washed" samples). The photoelectrodes were then prepared for fully sealed solar cells (see the Experimental section) and their optical transmittance and absorptance (Fig. 2a–d), dye loading (Fig. 3a) and photovoltaic performance (Fig. 4a–f) were measured. Reference samples were prepared using the conventional "rapid sensitization" by spreading 70–80 μL (175–200 μL cm^{-2}) of the same dye solution on an identical TiO_2 film using a pipette ("drop-cast" samples), followed by the same 15 minute settling and final rinsing as done for the washed inkjet-printed samples.

According to the optical characterization, five printing cycles were enough to achieve the coloration of the films close to that of the drop-cast samples, which we consider to be fully saturated with the dye. With 1–5 printing cycles, the device transmittance could be varied systematically from 38% to 8% (at 550 nm), while the photoelectrode absorptance ranged correspondingly from 44% to 88% (Fig. 2a and d and Fig. S3 in ESI†). This immediately

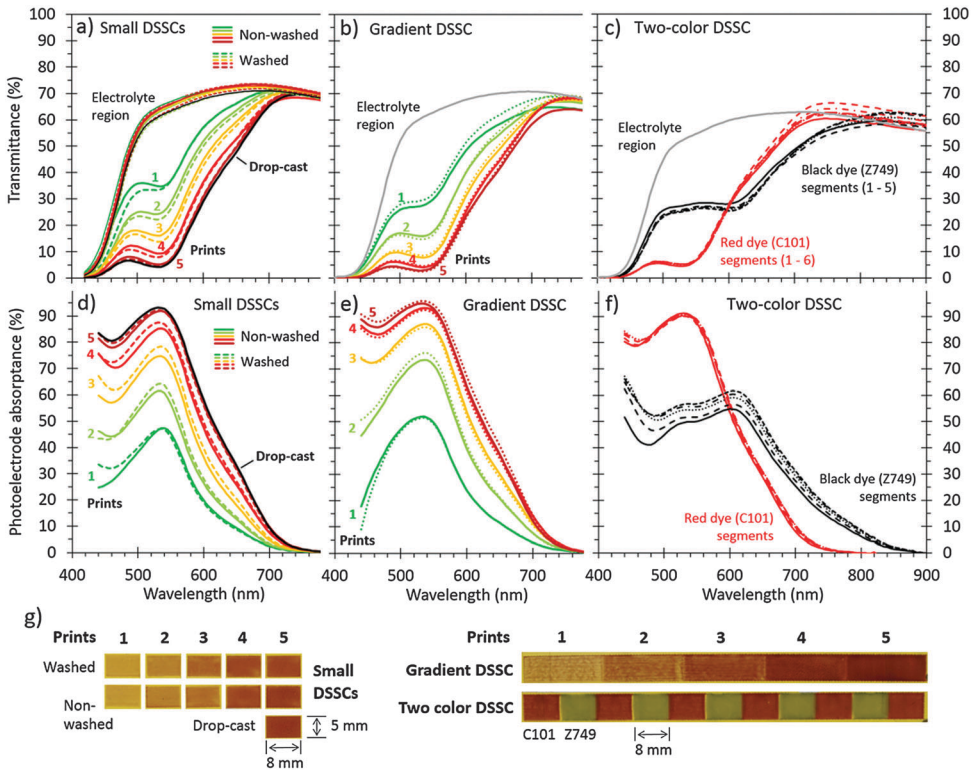

Fig. 2 Optical characteristics of semi-transparent DSSCs with inkjet-printed dyes: (a–c) transmittance, (d–f) photoelectrode absorbance, (g) photographs. (a and d) Small DSSCs dyed by inkjet-printing a dye solution (10 mM C101 in DMF) 1–5 times (1.1 μL cm^{-2} per print) over a 7 μm thick TiO_2 electrode (0.4 cm^2, no scattering layer), followed by rising with DMF ("Washed") or omitting the rinsing ("Non-washed"), compared with a reference sample dyed by drop-casting 70–80 μL of the same dye solution on an identical TiO_2 film using a pipette, followed by the same washing treatment ("Drop-cast"). (b and e) A DSSC with color density gradient made by inkjet-printing the C101 dye solution 1–5 times over different parts of the same TiO_2 electrode. (c and f) A two-color DSSC with ink-jet printed red (C101) and black (N749) dye segments on the same TiO_2 electrode. (d–f) Show the internal absorbance spectra of the photoelectrode layer calculated as the ratio of the transmittances through the photoelectrode and electrolyte regions of the same cell (a–c), normalized to zero at long wavelengths (at 800 nm for C101 and 900 nm for N749); (g) photographs of the photoelectrode regions of the measured DSSCs taken with white backlight. The printing was done in all the cases with a 10 pL drop volume and 30 μm drop spacing, using 10 mM C101 in DMF as the red dye ink and 10 mM N749 in DMF as the black dye ink (printed in 5 cycles). The small DSSCs spectra shown are examples from the complete data set consisting of three samples of each type. The complete data set and details of the calculation of figures (d–f) are available in the ESI.†

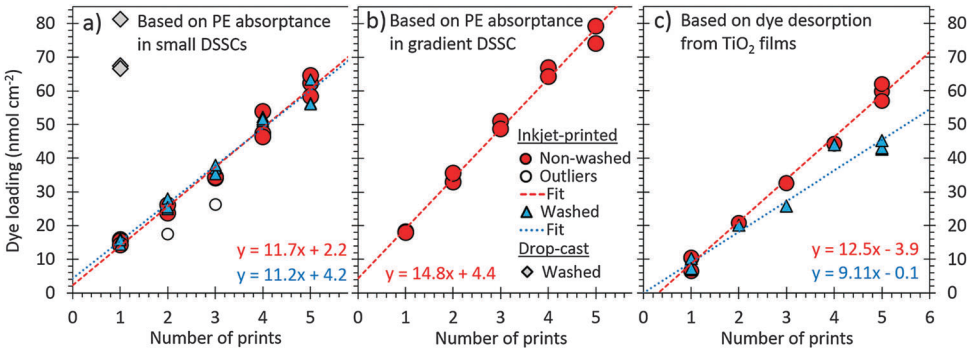

Fig. 3 Dye loading in the small DSSCs (a) and the gradient DSSC (b) determined from their photoelectrode absorbance spectra shown in Fig. 2, and confirmed by dye desorption from the TiO_2 films (c). The lines are linear fits to the data with equations shown. Note that many data points are overlapping. The number of data points are: (a) three for each 1–5 prints, (b) three for 1 and 3 prints and one for 2 to 4 prints, (c) two for each for each 1–5 prints. The data points marked as outliers in (a) correspond to the samples with less uniform coloration and are excluded from the fit. Details of the dye loading calculations are given in the ESI.†

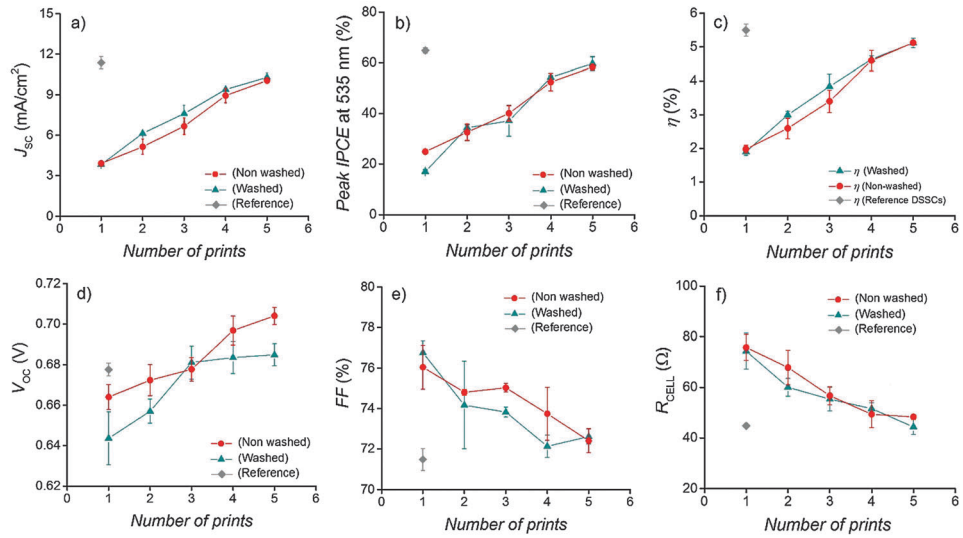

Fig. 4 (a–f) Photovoltaic parameters of one batch of DSSC devices with 1–5 time printed PEs. The points are average values of three cells and the error bars represent their standard deviation.

shows the unique feature of dye-sensitization using inkjet-printing that could be interesting for many applications of the semi-transparent DSSCs: the transparency of the devices can be fine-tuned by the dispensed amount of dye without changing the thickness of the TiO_2 film. This is exactly opposite to the conventional dyeing processes that produce fully dye-saturated films with transmittance dictated by their thickness.

The other interesting feature of inkjet printing already mentioned is that it allows printing almost arbitrary dye patterns (Fig. 1). Fig. 2g shows this capability in more detail by demonstrating the two most obvious opportunities it implies: the creation of dye patterns with varying color density ("gradient DSSC") and combinations of multiple dyes ("two-color DSSC") on the same photoelectrode. The optical characteristics of the five individual segments in the gradient DSSC, dyed with 1–5 prints of the C101 dye, are similar to those observed in the small individual DSSCs, but produced on the same long TiO_2 electrode stripe (Fig. 2b and e *vs.* Fig. 2a and d). In the two-color DSSC, the characteristic absorptance spectra of the printed red (C101) or black (N749) dyes can be distinguished from the adjacent segments without any signs of mixing between them (Fig. 2c and f). This shows that inkjet printing accurately fixed the dyes in their own segments, allowing multicolored dye patterns to be produced on the same electrode. Note how uniform the coloration is in each segment of the two-color DSSC (Fig. 2g), and how repeatable the color density is between them, especially for the red dye (Fig. 2c and f). Although the coloration is less uniform in the gradient DSSC with 1–3 prints, it improves substantially with the successive 4th and 5th prints, and is remarkably good in the small DSSCs, even with a single print, so that practically no visual difference can be seen between the five-time printed and drop-cast samples (Fig. 2g).

2.1.2. Precise control of dye loading. Washing the TiO_2 films after printing the dye affected neither their optical absorbance nor visual appearance (Fig. 2d and g), and no traces of the dye could be seen in the transmittance spectra recorded from the

free electrolyte region of the cells (Fig. 2a–c). This indicates that all the printed dye had attached well to the TiO_2 film, leaving no excess or loosely bound dye that could be removed by washing or released into the electrolyte when built into a DSSC, even when the washing step had been omitted. The dye loading in the TiO_2 films, estimated from the photoelectrode absorptance spectra as detailed in the ESI,† confirms this by showing excellent agreement between the washed and non-washed samples (Fig. 3a). Moreover, the dye loading increases linearly with the number of prints, demonstrating good control and repeatability of the printing process. The average dye loading per print determined from the slope of the linear fits is 11.2 nmol cm^{-2} in the washed and 11.7 nmol cm^{-2} in the non-washed samples, which matches almost perfectly with the dispensed amount (11.3 nmol cm^{-2}) determined by the printer settings (drop volume, spacing, and concentration). Note that the dye loading obtained with five prints (56–65 nmol cm^{-2}) is only slightly below the values achieved by drop-casting (68–81 nmol cm^{-2}), as one would expect if the loading does not exceed the saturation limit, but is close to it (Fig. 3a). Similar results with excellent linearity are also observed in the gradient DSSC, although at somewhat higher 14.8 nmol cm^{-2} loading per print (Fig. 3b). The relatively high values with five prints (74–79 nmol cm^{-2}), achieved without signs of saturation in the linear trend, indicate a somewhat higher film thickness in the gradient DSSC compared to the small DSSCs.

To confirm these results, some of the inkjet-dyed TiO_2 films from the same batch as those built into solar cells underwent a dye desorption experiment, where the printed dye was detached from the films to a desorption solution of known volume and then quantified using UV-VIS absorbance spectroscopy (see the Experimental section and ESI†). The results correspond well to those determined optically from the complete DSSCs: the dye loading increases linearly with the number of prints with slopes of 9.1 nmol cm^{-2} per print in the washed and 12.5 nmol cm^{-2} per print in the non-washed samples (Fig. 3c), and the values per film thickness obtained with five prints (6.5 and 8.9 nmol cm^{-2} μm^{-1}, respectively) are close to the values reported for the same dye by others (8.8 to 11.4 nmol cm^{-2} μm^{-1}).[33] Note that although the lower slope would suggest that washing had removed a significant amount of dye from the films in this case, only small amounts (<6 nmol cm^{-2}) were detected in the five-time printed samples using UV-VIS spectroscopy, and none in the samples printed 1–4 times (data not shown). We therefore consider that these lower loadings, which deviate from the general trend more than the normal variation, resulted from occasionally failed printing cycles, which occurred in less than 4% of all the 174 printing cycles constituting the results of Fig. 3a–c. Indeed, only four of the nine washed samples in Fig. 3c show results below the linear trend of the non-washed ones, whereas the rest match well with it.

2.1.3. Photovoltaic performance of the semi-transparent DSSCs. Also the results from the photovoltaic characterization show clear trends without any significant differences between washed and non-washed samples (Fig. 4). The short circuit photocurrent density (J_{SC}) increases systematically with the number of prints, reaching *ca.* ~10.1 mA cm^{-2} with five prints (Fig. 4a), which is slightly lower than in the drop-cast samples (*ca.* ~11.4 mA cm^{-2}), as expected from their lower dye loading (Fig. 3a). The peak value of incident-photon-to-collected-electron efficiency (IPCE) and the energy conversion efficiency (η) have similar trends to J_{SC}, reaching 59% and 5.1%, respectively with the fifth print, compared to 65% and 5.5% by drop-casting (Fig. 4b and c). This shows that dye loading (light absorption) was the main performance determining factor of these cells, which is also reflected in the other *JV* characteristics: When more dye is printed on the TiO_2 film of fixed thickness, the open circuit voltage (V_{OC}) increases (Fig. 4d), because more photocurrent is generated per unit volume of the film while the recombination rate ('dark current') remains more or less constant. The same would happen if the light intensity was increased instead.[34] Finally, the fill factor (FF) and cell resistance (R_{CELL}) follow qualitatively what is expected based on the evolution of J_{SC} and V_{OC} according to the electrochemical device model of DSSCs:[34] the decrease of FF (Fig. 4e) follows the increase of J_{SC}, because the voltage losses caused by the internal cell resistances at the maximum power increase proportionally to the current density, whereas the dependence of V_{OC} on the photocurrent is weaker (logarithmic). On the other hand, the observed reduction of R_{CELL} (Fig. 4f) with the increasing number of prints is expected based on the concomitant increase in V_{OC} (Fig. 4d), because the recombination resistance of the photoelectrode, which is the main contributor to R_{CELL} at the open circuit, is a decreasing function of voltage.[34]

Short circuit current densities measured from the individual segments of the gradient and two-color DSSCs show a synergic operation that is expected from their electrical parallel connection in the cell: the lower J_{SC} of the more transparent segments are compensated by the higher J_{SC} from the darker segments, so that their average is close to the value measured for the solar cell as a whole (Fig. 5). Note that the J_{SC} values of the five-time printed red segments in both cells are lower than in the small DSSCs (Fig. 4a), although their optical absorption is similar (Fig. 2d–f). This is at least partly due to the difficulty of establishing comparable measurement conditions when most of the active area in the large cells has to be masked when the individual segments are measured. It also creates a situation where the results correspond to the parallel connection of illuminated and dark segments, making detailed *JV* analysis not feasible.

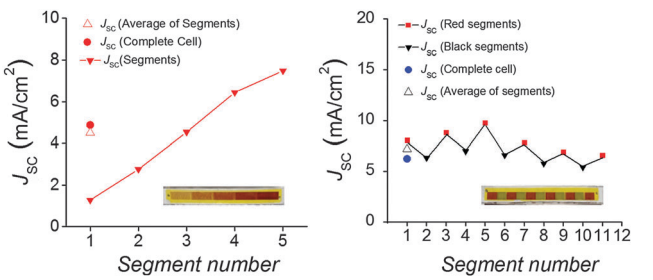

Fig. 5 J_{SC} characteristics of the gradient and two-color DSSCs.

2.2. Verification of high performance and stability of the inkjet-dyed DSSCs

Keeping all the above advantages and capabilities of dye-sensitization by inkjet printing in mind, it was confirmed that it is also entirely applicable for the preparation of traditional, non-transparent, high-efficiency DSSC designs. For this purpose, photoelectrodes consisting of an ~12 μm thick mesoporous TiO_2 layer and a 4–6 μm thick light scattering TiO_2 layer (0.8 × 0.5 cm^2 PE area) were sensitized by dispensing 5 ± 1 μL volume through 5 prints, which exhibited very minor impressions of the excess dye over the TiO_2 scattering layer, and were not rinsed further with the solvent.

The complete DSSCs were fabricated with these dye-printed photoelectrodes by employing a sulfolane – ionic liquid electrolyte (coded as Z988)[6] as the redox mediator along with platinum (Pt) counter electrodes, and their initial and long term stability performance was compared with the reference DSSCs, which were fabricated by drop casting the known volumes (70–80 μL with 20–25 minute settling) of concentrated (10 mM in DMF) solution of the C101 dye over the similar PEs, followed by washing with DMF, using current–voltage (*JV*) analysis, electrochemical impedance spectroscopy (EIS) and incident photon to collected electron (IPCE) measurements.

Statistical analysis of the average initial performance of seven dye-printed DSSCs (efficiency 6.4 ± 0.3%) and five reference DSSCs (6.2 ± 0.4%) showed no statistically significant difference between the two groups for any of the *JV* or EIS parameters (Tables S1 and S4 in the ESI,† respectively). Most importantly, the two types of DSSCs showed almost equal short circuit current densities (14.0 ± 0.2 mA cm^{-2} for printed dye and 13.8 ± 0.3 mA cm^{-2} for reference DSSCs), which confirms the successful sensitization process through inkjet printing.

The best performing devices among printed dye based DSSCs (five cells) and reference DSSCs (three cells) were then monitored through an accelerated ageing test at 35 °C along with 1 Sun illumination over a period of 1000 hours (see the Experimental section and ESI† for further details). Fig. 6a–e shows the ageing trends of the photovoltaic parameters that were collected from periodic measurements during the 1000 h test, and the initial and aged *JV* and IPCE curves of the best DSSCs of each type are shown in Fig. 7 and 8, respectively. The results reveal highly stable performance retained at almost 100% of the initial conversion efficiency (η = 6.4 ± 0.2%) and short circuit current density (J_{SC} = 14.2 ± 0.6 mA cm^{-2}) values, with no statistically significant ageing of any of the *JV* parameters of each cell type, according to a paired Student's *t*-test at 95% confidence (see ESI†). This was also confirmed using periodic electrochemical impedance spectroscopy measurements performed throughout the ageing test, which revealed high stability with no statistically significant changes in any of the internal resistance components of the DSSC (Fig. 9a and b, see the ESI† for detailed results). The only statistically significant difference observed was a 5% lower V_{OC} in the printed cells compared to the reference cells at the end of the aging period (1000 h, ESI,† Table S2), and the corresponding 14% lower recombination resistance in the printed cells, as measured by

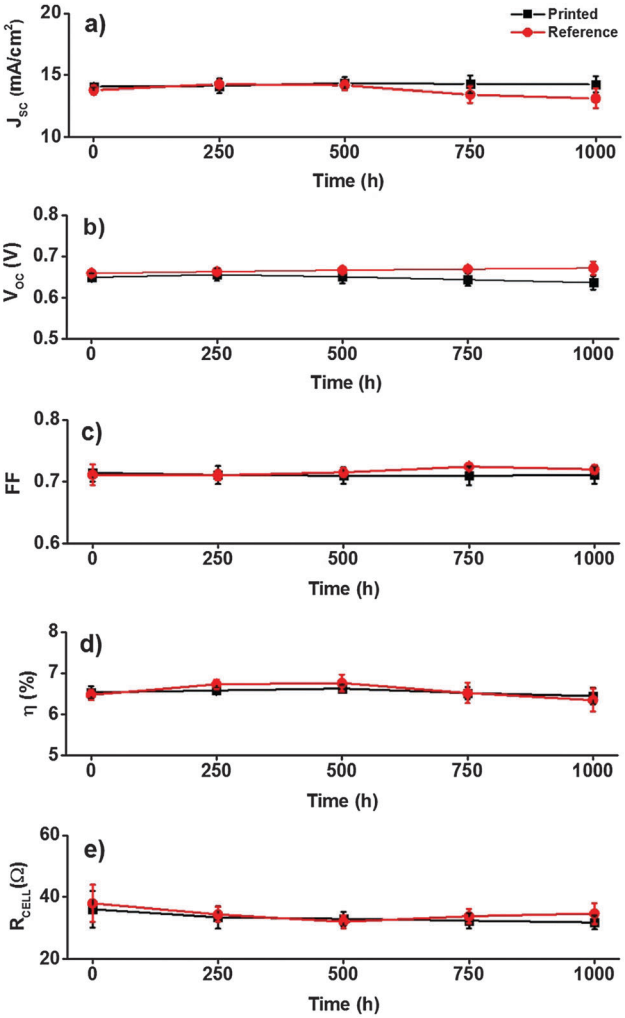

Fig. 6 (a–e) Photovoltaic parameters of fabricated devices of each type of DSSC obtained using periodical measurements during an accelerated ageing test (at 35 °C under 1 Sun illumination) for a period of 1000 hours. The points are average values of five printed and three reference (drop-cast) cells, and the error bars represent standard deviation.

EIS at V_{OC} (Table S5, ESI†). This points to a small difference in the aging behavior of the TiO_2/dye/electrolyte interface, which however, due to a compensating evolution of J_{SC} (Fig. 6d), resulted in no difference in the overall efficiency (Fig. 6d). Very small impressions of the excess dye that had remained over the scattering TiO_2 layer after the dye printing step, slowly dissolved into the electrolyte during the accelerated ageing test, which however caused no effects on the overall cell performance.

Encouraged by the first promising long term stability test, the same dye printed DSSCs (five cells) were further subjected to an additional accelerated test that was conducted under half Sun illumination at higher temperature (60 °C) for 1154 more hours (to test if a higher temperature could affect the performance). Again, the solar cells exhibited stable performance retaining almost 100% of the initial conversion efficiency (Fig. 10a–d). Hence these two ageing tests certify the potential of inkjet printing as a new sensitization process for DSSCs which is expected to be developed further after these results.

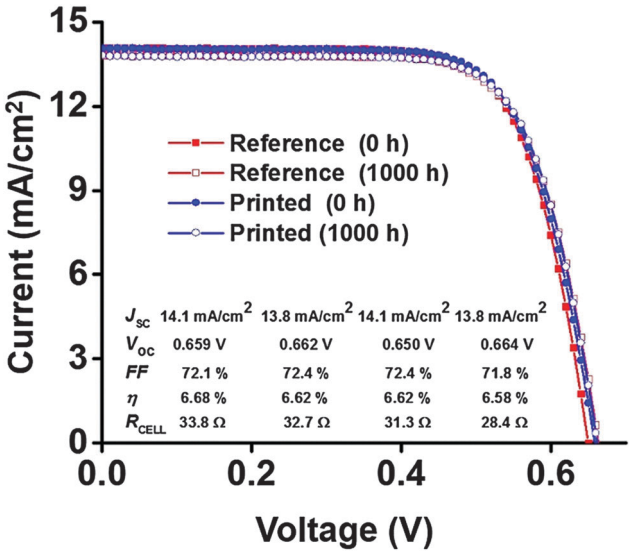

Fig. 7 Initial and aged (at 35 °C under 1 Sun illumination) *JV* curves of the best DSSCs of each type used in this study.

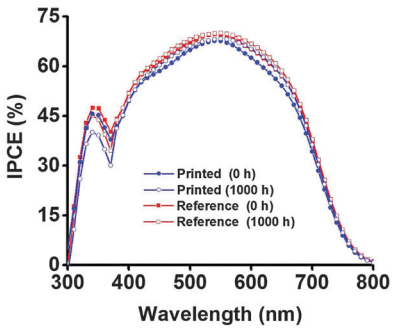

Fig. 8 Initial and aged (at 35 °C under 1 Sun illumination) IPCE spectra of the best DSSCs of each type used in this study.

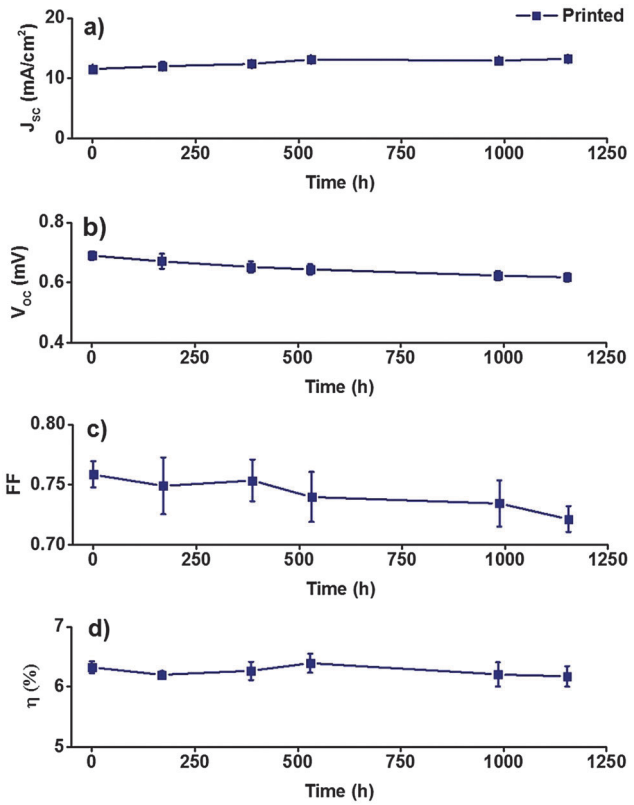

Fig. 10 (a–d) Average photovoltaic parameters of five printed DSSCs along with their standard deviations obtained by periodical measurements during an accelerated ageing test (at 60 °C and half Sun illumination) for 1184 hours.

In addition to the main capabilities of inkjet printing the dye discussed earlier, namely, the controlled dispensing and patterning of the dye, several other possible advantages can be mentioned. For instance, the highly pure dye solution can be contained in the printer cartridge until dispensed on the active layer, which protects it from contamination or degradation. Since the dye is printed only on the active layer, additional cleaning steps to remove the dye from the non-active area around it, before the application of the thermoplastic sealants, are not necessary. For the same reason, inkjet printing may also be potentially beneficial for plastic photoelectrodes, because it provides an opportunity to minimize the contact and interaction

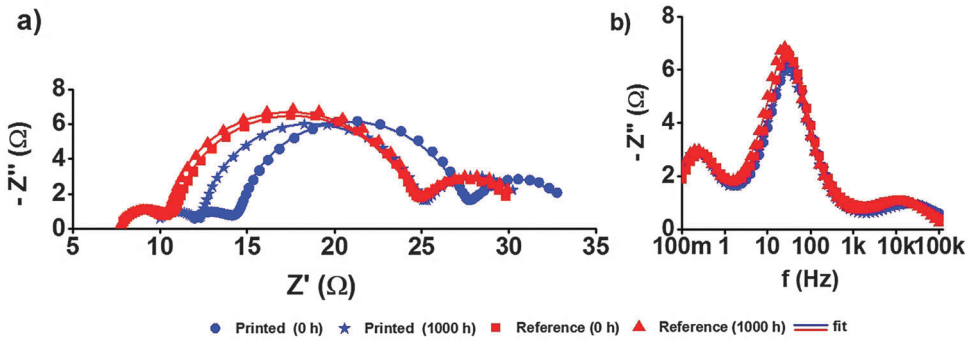

Fig. 9 Typical fresh and aged EIS spectra of complete DSSCs of the best devices of each type used in this study with a Pt counter electrode (a) Nyquist plots, (b) imaginary impedance (*Z*″) *vs.* frequency. The solid lines represent the fitted data, whereas the points represent the measured data. The shift of the Nyquist plot along the real axis in the case of printed dye DSSCs was due to a gradual decrease in the contact (series) resistance of the silver paint during the aging test.

of possibly harsh solvents with plastic substrates, such as the commonly used indium doped tin oxide coated polyethylene terephthalate (ITO-PET) and polyethylene naphthalate (ITO-PEN) sheets. For example, ITO-PET might swell when exposed to certain solvents such as acetonitrile for long time periods required in the traditional dye bath soaking process. Hence, we also aim to apply and investigate this technique on flexible PEs in future. Again, unlike in the dye circulation process used for sensitizing the hermetically pre-sealed modules, in inkjet printing the dye solution never comes in contact with the Pt catalyst, which may help keep it clean of adsorbed dye molecules that could lower its catalytically active surface area. Moreover, the inkjet printing of dyes can also be potentially utilized for more accurate and controlled co-sensitization of TiO_2 layers by multiple dyes, by printing them at optimized amounts over the same electrode area, instead of controlling only the soaking time, which is the traditional approach.

3. Conclusion

In conclusion, the TiO_2 photoelectrodes of dye-sensitized solar cells (DSSCs) can be effectively stained by inkjet printing concentrated dye solutions on them. The unique feature of inkjet printing is that it allows accurate control of dye loading with respect to both the amount and position on the TiO_2 film. This offers several advantages over the conventional dye application methods. First, close to full coloration can be achieved without rinsing off any excess dye, which simplifies the DSSC fabrication process and reduces material consumption. Second, the color density of the films can be tuned without changing their thickness, which offers a new degree of freedom in the design of semi-transparent DSSCs, for example, for building integrated photovoltaics. Third, the high spatial resolution of inkjet printing makes it possible to create color density gradients and patterns of multiple dyes on the same photoelectrode, which suggests a new avenue for creating multi-colored DSSC designs attractive, for example, for stylish product integration of DSSCs. The inkjet printing of dyes is applicable with or without a light scattering TiO_2 layer, and yields stable devices with performance equal to those prepared using the manual drop casting sensitization process. Since inkjet printing is one of the most well-known, established and scalable techniques for manufacturing printed electronics, this new dye-sensitization process could be readily adopted in the industrial settings, possibly even in the high throughput roll-to-roll production of flexible DSSC devices. Combined with our previously reported inkjet printing of electrolytes,[36] the results presented here show a path towards fully inkjet-printed DSSCs.

4. Experimental

Materials

Chloroplatinic acid hydrate ($H_2PtCl_4{\cdot}6H_2O$, purity 99.9%), guanidine thiocyanate (GuSCN, purity >99%), 1-methylbenzimidazole (NMBI, purity 99%), all the solvents (sulfolane 99% purity, 2-propanol 99.5% anhydrous, acetonitrile 99.8% anhydrous, *N*,*N*-dimethylformamide (DMF) 99.8% purity) and the titanium(IV) chloride tetrahydrofuran complex were obtained from Sigma Aldrich. 1,3-Dimethylimidazolium iodide (DMII), 1-methyl-3-propylimidazolium (PMII >98% purity), 1-ethyl-3-methylimidazolium iodide (EMII >98% purity) and 1-ethyl-l-3-methylimidazolium tetracyanoborate (EMITCB) were purchased from Merck. TiO_2 nanocrystalline paste (18-NRT, 20 nm) and TiO_2 scattering paste (WER 2–0, 400 nm) were purchased from Dyesol. Dye C101 and electrolyte Z988 were produced as reported earlier.[6,32,35] Dyes N749 and SQ2 were obtained from Solaronix, whereas dye Z907 was purchased from Dyesol. Solvent dimethyl sulfoxide (DMSO, ultra-pure grade) was purchased from Amresco.

TiO_2 photoelectrodes (PE)

The photoelectrodes for this experiment were prepared as follows. Fluorine doped tin oxide (FTO) coated NSG-Glass substrates (area = 1.6 cm × 2.0 cm and sheet resistance 10 Ω sq^{-1}) were first washed and sonicated with a detergent (10 minutes). The substrates were further washed and sonicated with acetone and ethanol solvents (5 minutes each) and were dried with compressed air. These substrates were then placed and cleaned (15 minutes) in a UV-O_3 cleaner (Bioforce Nanosciences USA). After cleaning in a UV-O_3 chamber, the substrates were immersed in 40 mM $TiCl_4$ solution and heated (30 minutes) in a preheated programmable oven and were sequentially rinsed with deionized water (DIW) and ethanol and were again dried with compressed air. The TiO_2 layers (12 μm of nanocrystalline TiO_2 particles, 20 nm and 4 μm thick layer of scattering particles, 400 nm) were sequentially screen printed and sintered at 450 °C for 30 minutes in the programmable oven and were cooled down to room temperature. Then, the photoelectrodes were re-heated in the 40 mM $TiCl_4$ aqueous solution and were washed again with DIW and ethanol and were dried with compressed air. Then, the photoelectrodes were again sintered at 450 °C in the programmable oven and were cooled down before the dye sensitization step. Note that the photoelectrodes for the dye desorption test (Fig. 3a and b) and for the dataset of DSSCs presented in Fig. 4(a–f) were not subjected to any $TiCl_4$ treatment and were not having any scattering layers, but only the semi-transparent TiO_2 layer (thickness 7 μm).

Dye solution formulations for inkjet printing

In the case of red C101 and black N749 (Fig. 1a and 2–10) the dye solution was 10 mM in DMF. In the case of blue SQ2 and red Z907 dyes (Fig. 1b and c), stock solutions were prepared (for individual dye) by dissolving 45 mg of dyes (SQ2 or Z907) in 3 mL of solvent dimethyl sulfoxide (DMSO). Both DMF and DMSO were found to be suitable solvents for inkjet printing these dyes.

Details of inkjet printing of dyes

Dye printing was achieved using an automated inkjet printer (Fuji Film's Dimatix Material Printer, Model DMP-2800 Series, see Fig. S4 in the ESI†) by filling the concentrated dye solutions

(dye C101 and N749) into its polymer cartridge. Additionally, the cartridge is equipped with a so-called 'print head' which consists of 16 micro-channels (orifices) through which the solution was dispensed. In order to get good printing results, the dye solution was passed through a 0.2 μm filter as recommended in the operating instructions of the printer. The TiO_2 layers (actual area = 0.8 × 0.5 cm^2) without the scattering layer were sensitized with both dye solutions at 10 mM concentration using a 30 μm drop spacing leading 0.45 μL solution and 4.5 nmol of dye deposition per cycle. See Fig. 2 caption for more details. The cells which underwent the ageing study were assembled employing a scattering layer on nanocrystalline TiO_2 and they were processed with a 20 μm drop spacing corresponding to 1 μL solution and 16 nmol of dye per print from 16 mM solution. The printing process took around 3 and 2 minutes for 20 μm and 30 μm drop spacing respectively.

Photoelectrode sensitization for reference DSSCs

The TiO_2 layers of the photoelectrodes for the reference DSSCs were sensitized using a similar procedure as reported earlier for quick sensitization of dye C101.[33] In brief, the TiO_2 layers were completely covered by spreading the dye solution of known volumes (70 μL) with similar concentrations (10–16 mM of dye C101 dye in DMF) as used in the inkjet printing of the dye and were left for 20 minutes in a sealed plastic box. After that each photoelectrode was washed with DMF to remove the excess dye and was dried with compressed air before the cell assembly.

Counter electrodes (CE)

A drop (4 μL) of 10 mM chloroplatinic acid hydrate ($H_2PtCl_4 \cdot 6H_2O$) solution (in 2 propanol) was cast over pre-cleaned FTO coated glass substrates (TEC 7) and was fired at 410 °C for 20 minutes. After that all the electrodes were cooled down to room temperature and were placed in a tightly sealed plastic box prior to the final cell assembly.

Electrolyte composition

The ionic liquid electrolyte coded as Z988 with the following composition was used for this study: DMII/EMII/EMITCB/I_2/NMBI/GuSCN (molar ratio 12 : 12 : 16 : 1.67 : 3.33 : 0.67) mixed and diluted with 50% of sulfolane (v/v).

Cell assembly

The cell channel was defined by separating PE and CE through a thick (25 μm) Surlyn frame foil. The ionic liquid electrolyte was introduced into the cell channel through the drilled holes at the CE side. The cells were then sealed with 25 μm thick Surlyn foil and a thin glass cover. At last, the contacts were fabricated by applying the copper tape and quick drying silver paste at the non-active area of the electrodes.

Measurements

The *JV* curves of the DSSCs were recorded in a xenon lamp based solar simulator (Peccell Technologies, Japan, Model PEC-L01) under 1000 W m^{-2} light intensity calibrated to equivalent 1 Sun conditions using a reference solar cell (PV Measurements Inc.), by using a black tape mask (aperture area 0.17 cm^2). The electrochemical impedance spectra were recorded from 100 mHz to 100 kHz under open circuit conditions at 1000 W m^{-2} light intensity on a Zahner-Elektrik IM6 electrochemical workstation, and analyzed using Zview2 software (Scribner Associates Inc.) using the well-known equivalent circuit model of DSSCs.[34] The incident photon to collected electron efficiency (IPCE) and transmittance spectra were measured using a QEX7 spectral response measurement unit (PV Measurements Inc.) at near normal incidence without bias light. The first stability test of the solar cells was performed by keeping them for 1000 hours under open circuit conditions at 35 °C in a self-made solar simulator under 1 Sun light intensity provided through halogen lamps (Philips 13117) and a UV filter (Asmetec GmbH, 400 nm cut-off), while recording their *JV* curves periodically in the above-mentioned separate solar simulator (Peccell Technologies, Japan). The second stability test was executed in the Suntest CPS Plus system at 60 °C under half Sun light illumination and similar periodic measurements as mentioned above were performed to record the *JV* curves in the solar simulator. The dye loading (mol cm^{-2}) in complete solar cells was determined based on two transmittance measurements from each cell: one taken through the photoelectrode and one through the electrolyte filled edge region next to it. The dye loading in freshly sensitized TiO_2 films was determined by desorbing the dye in a mixed solution of TMAOH and DMF (50/50 by volume). The decadic molar attenuation coefficient of C101 dye (17.5 × 10^3 M^{-1} cm^{-1}) used in the calculations was taken from ref. 33. The details of both methods are given in the ESI.†

Acknowledgements

G. H. gratefully acknowledges the Academy of Finland for the post-doctoral research fellowship (Grant number: 287641). J. H. acknowledges the financial support from the Technology Industries of Finland Centennial Foundation (NIR-DSC project). M. G. acknowledges financial support from Swiss National Science Foundation and CTI 17622.1 PFNM-NM, glass2energy SA (g2e), Villaz-St-Pierre, Switzerland. This work was also supported by the SELECT + (Environomical pathways for sustainable energy services). Bioeconomy infrastructure is also acknowledged for the use of the equipment.

References

1 G. Hashmi, K. Miettunen, T. Peltola, J. Halme, I. Asghar, K. Aitola, M. Toivola and P. Lund, *Renewable Sustainable Energy Rev.*, 2011, **15**, 3717–3732.
2 A. Feltrin and A. Freundlich, *Ren. Energy*, 2006, **33**, 180–185.
3 C. S. Tao, J. Jiang and M. Tao, *Sol. Energy Mater. Sol. Cells*, 2011, **95**, 3176–3180.
4 A. Hinsch, W. Veurman, H. Brandt, K. Flarup Jensen and S. Mastroianni, *ChemPhysChem*, 2014, **15**, 1076–1087.
5 K. Zhang, C. Qin, X. Yang, A. Islam, S. Zhang, H. Chen and L. Han, *Adv. Energy Mater.*, 2014, **4**, 1301966.

6 M. Marszalek, F. D. Arendse, J. D. Decoppet, S. S. Babkair, A. A. Ansari, S. S. Habib, M. Wang, S. M. Zakeeruddin and M. Grätzel, *Adv. Energy Mater.*, 2014, **4**, 1301235.
7 Z. L. Wang and W. Wu, *Angew. Chem.*, 2012, **51**, 2–24.
8 F. De Rossi, T. Pontecorvo and T. M. Brown, *Appl. Energy*, 2015, **156**, 413–422.
9 S. Vignati, MSc thesis, Comm. Syst. Dept., KTH, 2012.
10 S. Ito, T. N. Murakami, N. Takurou, P. Comte, P. Liska, C. Graetzel, M. K. Nazeeruddin and M. Graetzel, *Thin Solid Films*, 2008, **516**, 4613–4619.
11 M. K. Nazeeruddin, A. Kay, I. Rodicio, R. Humphry-Baker, E. Mueller, P. Liska, N. Vlachopoulos and M. Graetzel, *J. Am. Chem. Soc.*, 1993, **115**, 6382–6390.
12 M. Hösel, H. F. Dam and F. C. Krebs, *Energy Technol.*, 2015, **3**, 293–304.
13 J. E. Carle, M. Helgesen, M. V. Madsen, E. Bundgaard and F. C. Krebs, *J. Mater. Chem. C*, 2014, **2**, 1290–1297.
14 D. Angmo, S. A. Gevorgyan, T. T. L. Olsen, R. R. Søndergaard, M. Hösel, M. Jørgensen, R. Gupta, G. U. Kulkarni and F. C. Krebs, *Org. Electron.*, 2013, **14**, 984–994.
15 J. S. Yu, I. Kim, J. S. Kim, J. Jo, T. T. L. Olsen, R. R. Søndergaard, M. Hosel, D. Angmo, M. Jørgensen and F. C. Krebs, *Nanoscale*, 2012, **4**, 6032–6040.
16 J. Adams, G. D. Spyropoulos, M. Salvador, N. Li, S. Strohm, L. Lucera, S. Langner, F. Machui, H. Zhang, T. Ameri, M. M. Voigt, F. C. Krebs and C. J. Brabec, *Energy Environ. Sci.*, 2015, **8**, 169–176.
17 K. Liu, T. T. Larsen-Olsen, Y. Lin, M. Beliatis, E. Bundgaard, M. Jørgensen, F. C. Krebs and X. Zhan, *J. Mater. Chem. A*, 2016, **4**, 1044–1051.
18 M. K. Nazeeruddin, R. Splivallo, P. Liska, P. Comte and M. Grätzel, *Chem. Commun.*, 2003, 1456–1457.
19 I. Concina, E. Frison, A. Braga, S. Silvestrini, M. Maggini, G. Sberveglieri, A. Vomieroa and T. Carofiglio, *Chem. Commun.*, 2011, **47**, 11656–11658.
20 P. J. Holliman, M. L. Davies, A. Connell, B. V. Velasco and T. M. Watson, *Chem. Commun.*, 2010, **46**, 7256–7258.
21 M. Späth, P. M. Sommeling, J. A. M. van Roosmalen, H. J. P. Smit, N. P. G. van der Burg, D. R. Mahieu, N. J. Bakker and J. M. Kroon, *Prog. Photovoltaics*, 2003, **11**, 207–220.
22 R. Sastrawan, J. Beier, U. Belledin, S. Hemming, A. Hinsch, R. Kern, C. Vetter, F. M. Petrat, A. P. Schwab, P. Lechner and W. Hoffmann, *Sol. Energy Mater. Sol. Cells*, 2006, **90**, 1680–1691.
23 Y. Seo and J. H. Kim, *J. Ind. Eng. Chem.*, 2013, **19**, 488–492.
24 H. Seo, M. K. Son, I. Shin, J. K. Kim, K. J. Lee, K. Prabakar and H. J. Kim, *Electrochim. Acta*, 2010, **55**, 4120–4123.
25 H. G. Han, H. C. Weerasinghe, K. M. Kim, J. S. Kim, Y. B. Cheng, D. J. Jones, A. B. Holmes and T. H. Kwon, *Sci. Rep.*, 2015, **5**, 14645.
26 B. Kim, S. W. Park, J. Y. Kim, K. Yoo, J. Ah Lee, M. W. Lee, D. K. Lee, J. Y. Kim, B. S. Kim, H. Kim, S. Han, H. J. Son and M. J. Ko, *ACS Appl. Mater. Interfaces*, 2013, **5**, 5201–5207.
27 R. Sastrawan, J. Beier, U. Belledin, S. Hemming, A. Hinsch, R. Kern, C. Vetter, F. M. Petrat, A. P. Schwab, P. Lechner and W. Hoffmann, *Prog. Photovoltaics*, 2006, **14**, 697–709.
28 S. G. Hashmi, T. Moehl, J. Halme, Y. Ma, T. Saukkonen, A. Yella, F. Giordano, J. D. Decoppet, S. M. Zakeeruddin, P. Lund and M. Gratzel, *J. Mater. Chem. A*, 2014, **2**, 19609–19615.
29 S. C. Yeh, P. H. Lee, H. Y. Liao, Y. Y. Chen, C. T. Chen, R. J. Jeng and J. J. Shuye, *ACS Sustainable Chem. Eng.*, 2015, **3**, 71–81.
30 Fig. 1e is reprinted from, H. Arakawa, T. Yamaguchi, T. Sutou, Y. Koishi, N. Tobe, D. Matsumoto and T. Nagai, Efficient dye-sensitized solar cell sub-modules, *Curr. Appl. Phys.*, 2010, **10**(2), S157–S160, with permission from Elsevier.
31 Fig. 1f is reprinted from, H. Pettersson, T. Gruszecki, C. Schnetz, M. Streit, Y. Xu, L. Sun, M. Gorlov, L. Kloo, G. Boschloo, L. Haggman and A. Hagfeldt, Parallel-connected monolithic dye-sensitised solar modules, *Prog. Photovoltaics*, 2010, **18**, 340–345, with permission from John Wiley and Sons.
32 F. Gao, Y. Wang, D. Shi, J. Zhang, M. Wang, X. Jing, R. H. Baker, P. Wang, S. M. Zakeeruddin and M. Gratzel, *J. Am. Chem. Soc.*, 2008, **130**, 10720–10728.
33 M. Wang, S. Plogmaker, R. H. Baker, P. Pechy, H. Rensmo, S. M. Zakeeruddin and M. Gratzel, *ChemSusChem*, 2012, **5**, 181–187.
34 J. Halme, P. Vahermaa, K. Miettunen and P. Lund, *Adv. Mater.*, 2010, **22**, E210–E234.
35 J. D. Decoppet, T. Moehl, S. S. Babkair, R. A. Alzubaydi, A. A. Ansari, S. S. Habib, S. M. Zakeeruddin, H. W. Schmidt and M. Gratzel, *J. Mater. Chem. A*, 2014, **2**, 15972–15977.
36 S. G. Hashmi, M. Ozkan, J. Halme, K. Dimic-Misic, S. M. Zakeeruddin, J. Paltakari, M. Grätzel and P. D. Lund, *Nano Energy*, 2015, **17**, 206–215.

